Machine learning assisted dual-channel carbon quantum dots-based fluorescence sensor array for detection of tetracyclines

Zijun Xu, Zhaokun Wang, Mingyang Liu, Binwei Yan, Xueqin Ren, Zideng Gao

PII: S1386-1425(20)30124-4

DOI: https://doi.org/10.1016/j.saa.2020.118147

Reference: SAA 118147

To appear in: *Spectrochimica Acta Part A: Molecular and Biomolecular Spectroscopy*

Received date: 17 December 2019

Revised date: 6 February 2020

Accepted date: 9 February 2020

Please cite this article as: Z. Xu, Z. Wang, M. Liu, et al., Machine learning assisted dual-channel carbon quantum dots-based fluorescence sensor array for detection of tetracyclines, *Spectrochimica Acta Part A: Molecular and Biomolecular Spectroscopy*(2020), https://doi.org/10.1016/j.saa.2020.118147

Machine learning assisted dual-channel carbon quantum dots-based fluorescence sensor array for detection of tetracyclines

Zijun Xu[†], Zhaokun Wang[†], Mingyang Liu[†], Binwei Yan[†], Xueqin Ren*[†‡], Zideng Gao*[†]

Authors affiliations

College of Resources and Environmental Sciences, China Agricultural University, Beijing

100193, PR China.

Address:

Beijing Key Laboratory of Farmland Soil Pollution Prevention and Remediation, China Agricultural University, Beijing 100193, PR China.

College of Resources and Environmental Sciences, China Agricultural University, 2#Yuanmingyuan west road, Haidian, Beijing, China, 100193.

*Corresponding author:

Zideng Gao. Email: gzdsch@163.com

Xueqin Ren. Email: renxueqin@cau.edu.cn

Tel: +86–010–6273–4468

Fax: +86–010–6273–4468

Zideng Gao and Xueqin Ren are co-corresponding author

ABSTRACT

The detection and differentiation of tetracyclines (TCs) has received increasing attention due to the severe threat they pose to human health and the ecological balance. A dual-channel fluorescence sensor array based on two carbon quantum dots (CDs) was fabricated to distinguish between four TCs, including tetracycline (TC), oxytetracycline (OTC), doxycycline (DOX), and metacycline (MTC). A distinct fluorescence variation pattern (I/I_0) was produced when CDs interacted with the four TCs. This pattern was analyzed by LDA and SVM. This was the first time that SVM was used for data processing of fluorescence sensor arrays. LDA and SVM showed that the array has the capacity for parallel and accurate determination of TCs at concentrations between 1.0 μM and 150 μM. In addition, the interference experiment using metal ions and antibiotics as possible coexisting interference substances proves that the sensor array has excellent selectivity and anti-interference ability. The array was also used for the accurate detection and identification of TCs in binary mixtures, and furthermore, the four TCs were successfully identified in river water and milk samples. Besides, the sensor array successfully identified the four TCs in 72 unknown samples with a 100% accuracy. The results proved that SVM can achieve the same accurate classification and prediction as LDA, and considering its additional advantages, it can be used as an optional supplementary method for data processing, thereby expanding the data processing field.

Keywords: carbon quantum dots, linear discriminant analysis, support vector machine, sensor array, tetracyclines

1. Introduction

Carbon quantum dots (CDs) is a new type of fluorescent carbon nanomaterial that is extensively researched in recent years. CDs are quasi-spherical nanoparticles with a particle size smaller than 10 nm[1]. There are abundant polar functional groups on the surface of these materials[2], which result in good water solubility. In addition, the methods of preparing CDs can be divided into top-down (including hydrothermal treatment[2, 3], arc discharge, electrochemistry, etc.) and bottom-up methods (including high temperature pyrolysis[4], combustion and microwave[5], etc.). Compared with traditional semiconductor quantum dots such as CdTe and CdSe, CDs have the advantages of low toxicity[6], wide source of raw materials, low cost[7], and good biocompatibility[8]. Therefore, CDs have been used in biological imaging[9], sensing detection, photoelectric conversion, photocatalysis[10] and other fields. The sensing detection application is one of the most promising fields. The high photostability ensures stable fluorescence signals and accurate detection results.

In order to further broaden these advantages, CDs are considered for the manufacture of multi-channel sensor arrays. Array sensing detection has numerous advantages, including accuracy, diversity, and the ability to simultaneously detect and distinguish a series of analytes with similar structures and properties. Examples of analytes are thiols[11], catecholamine neurotransmitters[12], nitroaromatic explosives[13, 14], benzaldehyde derivatives[15] and so on. However, the analysis and processing methods of multidimensional data obtained with array detection still

need to be modified and improved. At present, principle component analysis (PCA) and linear discriminant analysis (LDA) are used for data processing. However, PCA may ignore internal classification information of data, resulting in undesirable classifications[16]. LDA is part of supervised learning dimension reductions[17], which can overcome this disadvantage and effectively solve the problem of linear classifications. Meanwhile, linear dimensionality reduction methods such as PCA and LDA employed the global Euclidean structure of the original data. For nonlinear data, it is impossible to accurately describe the true distance between any two data points. Therefore, PCA and LDA have limitations in solving linear inseparable and nonlinear classification problems. Support vector machine (SVM) is an algorithm suitable for processing small sample data in both linear and nonlinear classification problems[18]. It is successfully applied in many fields of pattern recognition, such as face recognition, financial risk assessment, gene recognition[19-21]. We introduced, for the first time, SVM to process array sensing detection data, in order to offer the optional data processing methods to researchers.

TCs are a class of broad-spectrum antibiotics, which play an important role in the treatment of bacterial infections, the diagnosis of malignant tumors, inhibiting the outbreak of animal diseases, promoting animal growth and many other areas[22, 23]. However, the disproportionate global use of TCs led to their excessive accumulation in the natural environment, and these residues will eventually enter the human body through water and food, endangering human health[24]. More seriously, residues may

also promote bacterial resistance to antibiotics, thereby disrupting the balance of ecosystems. Based on these potential hazards, the detection of TCs in natural water and food is of great concern to researchers worldwide. Over the past few decades, great effort has been devoted to develop sensitive and selective detection and identification techniques for antibiotics, such as radioimmunoassays, enzyme-linked immunosorbent assays[25], fluorescence and phosphorescence methods, thin layer chromatography, high performance liquid chromatography (HPLC)[26], and liquid chromatography-mass spectrometry (LC-MS). However, these techniques have their own shortcomings, such as time-consuming, low resolution and sensitivity, complex detection process and expensive instruments[27, 28]. Array sensing detection may be a suitable alternative, but very few sensor arrays have been reported for the detection of TCs up to now. It is therefore essential to develop a sensitive, low-cost, simple and rapid TCs detection method.

Considering the importance and difficulty of detecting TCs, in this work, we selected two CDs to design a dual-channel fluorescence sensor array based on inner filter effect (IFE) to distinguish between four TCs, including TC, OTC, MTC and DOX. The two CDs were synthesized using only quinaldine red (QR) and cetylpyridinium chloride (CPC) as raw materials, abbreviated as QR-CDs and CPC-CDs, respectively. Due to the good overlapping areas between the TCs absorption spectra and excitation spectra of QR-CDs and CPC-CDs, effectively fluorescence quenching occurred, as analytes were added to the system. According to

the distinguished fluorescence intensity variations I/I_0 (I and I_0 represent the fluorescence intensity in the presence and absence of TCs, respectively) of the two CDs, a fluorescence analysis pattern was created for each analyte. The multidimensional data were analyzed and processed by LDA and SVM. The four TCs of different concentrations were successfully separated and differentiated adequately in binary TCs mixtures. Regarding practical applications, the identification of TCs in complex media (river water and milk) was validated. The sensor array also identified total 72 unknown samples with 100% accuracy. To the best of our knowledge, SVM was, for the first time used in this study to analyze multidimensional data of a CDs-based sensor array. This fluorescence sensor array could be more widely applied to detect and identify other pollutants with similar chemical structures and properties.

2. Experimental

2.1. Reagents and materials

Tetracycline (TC), oxytetracycline (OTC), doxycycline (DOX), metacycline (MTC), sulfadimethoxine sodium salt (SMM), tobramycin (TOB), amikacin (AMK), enrofloxacin (ENR), quinaldine red (QR), cetylpyridinium chloride monohydrate (CPC), trichloroacetic acid (TCA), and dichloromethane (CH_2Cl_2) were purchased from Aladdin Industrial Corporation (Shanghai, China). NaOH, HCl, anhydrous $CaCl_2$, $AgNO_3$, NaCl, LiCl, $Hg(NO_3)_2$, $CuSO_4·5H_2O$, $CdCl_2·2.5H_2O$, $MgCl_2·6H_2O$, $ZnSO_4·7H_2O$ and $BaCl_2·2H_2O$ were purchased from Sinopharm Chemical Reagent Co., Ltd. (Shanghai, China). All chemicals were of analytical grade and used as received without further purification. Deionized water was supplied by China Agricultural University (Beijing, China). A dialysis bag (MWCO 3000 Da) was purchased from Biotopped Technology Co., Ltd (Beijing, China).

2.2. Preparation of QR-CDs and CPC-CDs

QR-CDs and CPC-CDs were synthesized according to a slightly modified method reported previously[29, 30]. The two CDs were simply obtained using QR and CPC as the carbon source. According to previous reports, the synthesis conditions, including NaOH concentration and reaction time, have a significant influence on the fluorescence intensity, water solubility and stability of the CDs. To obtain the QR-CDs, 10 ml NaOH (1.0 M) was added to a QR aqueous solution (5 mM, 20 ml) and subsequently sonicated for 24 h in ice bath. The reaction was terminated by

adjusting the pH to neutral (pH 7.0) with hydrochloric acid (HCl). To obtain the CPC-CDs, 10 ml NaOH (330 mM) was transferred to an aqueous CPC solution (50 mM, 20 ml) and ultrasonication applied for 6 h in ice bath. Next, CH_2Cl_2 was added to the prepared reaction solutions and the upper layer of the aqueous phase separated. This layer was repeatedly extracted until the solution was completely colorless and transparent. The two CDs solutions were dialyzed against deionized water using a dialysis bag (MWCO membrane, 3000 Da) for 24 h to remove interfering substances. The two CDs were finally stored at 4 ℃ in a dark place.

2.3. Characterization

The fluorescence spectra were recorded using a fluorescence spectrophotometer (F-7000, Hitachi, Japan). The UV-vis spectra were acquired using a Tu-1810 UV-VIS spectrophotometer (General Analysis, China). Fluorescence lifetime measurements were carried out using an FLS 920 spectrometer (Edinburgh Instruments, U.K.). Fourier transform infrared (FT-IR) spectra were recorded on an iS10 Thermo Nicolet spectrometer (USA), with samples prepared using the KBr pellet method. X-ray photoelectron spectroscopy (XPS; Thermo Escalab 250Xi, USA)was acpuisited and processed by the advanced Avantage data system. High-resolution scanning/transmission electron microscopy (STEM; FEI Talos F200 series, 200kV) was used to obtain the morphology and microstructure of QR-CDs and CPC-CDs.

2.4. Array building procedure

The four TCs (TC, OTC, MTC, DOX) and the QR-CDs and CPC-CDs were used to prepare the detection system. TCs in various concentrations (0, 1.0 μM, 10 μM, 25 μM, 50 μM, 100 μM, 150 μM) were added to QR-CDs (10 ul, 13.3 μg mL^{-1}) and CPC-CDs (20 ul, 60 μg mL^{-1}), respectively. A sample volume of 1.0 ml was prepared and the detection conditions adjusted to a pH of 7.0. The sample was first incubated for 2 min, the fluorescence spectra of QR-CDs and CPC-CDs were recorded using excitation wavelengths of 320 nm and 370 nm, respectively. Five replicates were measured at each experimental condition. A training data matrix (2 CDs × 4 TCs × 5 replicates) was generated using I/I_0 values, and the data were further processed using LDA and SVM in R version 3.6.1. Then, the selectivity and anti-interference ability of the fluorescence sensor array were tested by replacing the four TCs with a series of commonly known interfering ions (Ca^{2+}, Cu^{2+}, Cd^{2+}, Mg^{2+}, Zn^{2+}, Hg^{2+}, Ag^{+}, Na^{+}, Ba^{2+}, and Li^{+}) and other possibly coexisting antibiotics (SMM, TOB, AMK, ENR). In addition, the TCs in the binary mixtures were analyzed. TC and DOX were selected to prepare the binary mixtures, and the total concentration of the two antibiotics maintained at 25 μM. The molar ratios of TC and DOX binary mixtures prepared were 0/100, 20/80, 40/60, 50/50, 100/0, respectively. The detection process was conducted the same way as for the single TCs. Finally, 52 unknown samples were studied to verify the reliability of the established fluorescence sensor array.

2.5. Preparation of real samples

River water and milk were selected as representative environmental samples. River water was collected from the Chaobai River (Beijing, China) and was pretreated according to reported methods[31]. After centrifuging the water samples at 12000 rpm for 5 min, impurities were removed, and the supernatant filtered with a 0.22 membrane. Subsequently, the four TCs spiked in the river water at the final concentration of 50 μM were distinguished by using the sensor array. The milk sample was purchased from a local supermarket (Beijing, China) and was pretreated according to reported methods[32, 33]. Briefly, trichloroacetic acid was poured into the milk and ultrasonication applied for 20 min. Then the proteins were separated and removed by centrifugation (12000 rpm, 10 min). Finally, the supernatant was filtered with a 0.22 membrane to remove impurities. The treated milk samples were diluted 50 times with deionized water. Then the four TCs with total concentrations of 25 μM and 50 μM were added to the samples for detection. The detection process was the same as that of the single TCs.

2.6. Statistical analysis

The array sensor detection data were analyzed and processed with LDA and SVM. LDA is a supervised learning dimension reduction and projects samples onto a straight line, so that the projections of similar samples are aggregated, and the projection points of different samples separated as far as possible. The model can be written as follows[34]:

$$J = \frac{w^T S_b w}{w^T S_w w} \quad (1)$$

where w is the direction vector, S_b is the inter-class divergence matrix and S_w is the intra-class divergence matrix.

SVM is a binary classification model, its purpose is to find a hyperplane to segment the sample. The principle of segmentation is to maximize the interval. The hyperplane equation is[35],

$$H(x) = w^T x + b \quad (2)$$

where w and x are the direction vectors.

The geometrical margin is as follows,

$$\gamma = \frac{|f(x)|}{||w||} = \frac{\gamma|f(x)|}{||w||} \quad (3)$$

where $f(x)$ is a classification model based on the hyperplane and w is the direction vector. Data analysis was implemented in R version 3.6.1.

3. Results and discussion

3.1. Preparation and characterization of QR-CDs and CPC-CDs

In this study, the two CDs used to construct a dual-channel fluorescence sensor array were prepared according to previous reports. The morphology, optical and structure properties of the two CDs were characterized including TEM, UV-vis absorption, fluorescence spectra, XPS, and FT-IR. TEM images of the prepared CDs, as shown in Figure 1, exhibited spherical structures and the mean diameter of the QR-CDs and CPC-CDs were estimated at 3.05 nm and 3.26 nm, respectively, on analyzing 105 individual particles. HRTEM images showed that both CDs have well-resolved lattice fringes, and the typical lattice spacing was 0.20 nm and 0.22 nm, respectively. The surface structures were investigated with FT-IR and XPS spectroscopy (Figure S2, S3). Based on the FT-IR and XPS spectral analyses, O-H/N-H structures at 3390 eV and 3460 eV on the surface of the CPC-CDs and QR-CDs were identified[36, 37], suggesting adequate water solubility. The N=C structures were also determined by the spectral bands at 1636.75 eV and 1384.23 eV on the surface of CPC-CDs and QR-CDs. XPS spectral analyses showed that three peaks related to C1s, N1s and O1s were identified at about 284.88, 401.1 and 532.52 eV for QR-CDs and 284.91, 401.65 and 531.58 eV for CPC-CDs, respectively[29].

Regarding the optical properties, QR-CDs and CPC-CDs were colorless solutions in ambient light but emitted strong blue and yellow fluorescence under irradiation with 312 nm and 365 nm UV light, respectively (Figure S4). The

maximum emission wavelengths were observed at 400 nm (QR-CDs) and 550 nm (CPC-CDs), at excitation wavelengths of 320 nm (QR-CDs), 340 nm and 380 nm (CPC-CDs). The quantum yields (QYs) measured in aqueous solution were 38% (QR-CDs) and 25.1% (CPC-CDs), referenced to Quinine sulfate (QY=0.557 in water) and Rhodamine B (QY=0.31 in water), respectively[38].

3.2. Sensor array detection mechanism

We proposed a fluorescence sensor array based on inner filter effect (IFE) for simple and sensitive detection of TCs. The IFE-based method does not require complex modification of CDs, nor any interaction between CDs and the analytes[39, 40], so it provides great flexibility and simplicity for the preparation of probes[41], and it is easier to realize the fluorescence sensing detection of pollutants.

In the sensor system, QR-CDs and CPC-CDs acts as fluorometric reporter and TCs function as the fluorescence absorber[42]. As shown in Figure S5, there are good overlapping areas between the absorption spectra of four TCs and excitation spectra of QR-CDs and CPC-CDs[40]. Therefore, when TCs were added to the two CDs, the fluorescence intensity of CDs can be effectively decreased. To further verify the principle, the UV-vis absorption spectrum of the two CDs (QR-CDs and CPC-CDs), four TCs (TC, OTC, MTC, DOX) and the mixture of them were measured, and calculated the quantitative addition of the UV absorption intensity of two CDs and four TCs. Figure S6 showed that the experimental curve (the absorption spectrum of CDs/TCs) are completely consistent with the theoretical curve (the physical addition

of the curves of CDs solution and TCs solution), indicating that no complex were formed between CDs and TCs[43]. In addition, the expected fluorescence lifetime is not affected by the IFE process[42]. As shown in Figure S7, S8, the existence of the four TCs do not affect the fluorescence lifetime of QR-CDs and CPC-CDs. This result further indicated that the fluorescence quenching of CDs can be attributed to the IFE between CDs and TCs.

3.3. Design and fabrication of the sensor array

The results demonstrated that the four TCs (TC, OTC, MTC, DOX) can effectively quench the fluorescence intensity based on IFE with QR-CDs and CPC-CDs. It was determined that the four TCs (TC, OTC, MTC, DOX) can effectively quench the fluorescence intensity of QR-CDs and CPC-CDs, but the quenching degree varies. The sensitivity of fluorescence quenching for each TCs can be correlated to quenching constant (K_{sv}), determined by the Stern-Volmer equation as follows[44],

$$I_0/I = 1 + K_{sv}[Q] \quad (4)$$

where K_{sv} represents the quenching efficiency of the TCs, and Q represents the analyte concentration. The Stern-Volmer constant were calculated to be 1.97×10^4 (TC), 3.65×10^4 (OTC), 1.39×10^4 (MTC), 1.15×10^4 (DOX) for QR-CDs and 4.69×10^4 (TC), 2.69×10^4 (OTC), 1.90×10^4 (MTC), 1.41×10^4 (DOX) for CPC-CDs, respectively. Thus, a dual-channel sensor array was fabricated in this study by monitoring the fluorescence changes of CDs. To achieve this goal, the fluorescence intensity

variation (I/I_0) of QR-CDs and CPC-CDs in the presence of TCs was investigated. This design and manufacturing process are illustrated in Scheme 1 and described briefly as follows. Firstly, the fluorescence response of the sensor array to a single analyte was tested to prove the capability of the sensor system. Then, the four TCs, with concentrations of 1.0 μM, were added to the two CDs. As a result, the fluorescence intensity of the two CDs was quenched, resulting in a slight red shift in the maximum emission wavelength. In preliminary experiments, the fluorescence responses of QR-CDs and CPC-CDs adding the four TCs (TC, OTC, MTC, DOX) were studied at concentrations between 1.0 μM and 150 μM. QR-CDs and CPC-CDs showed different quenching degrees, varying the TCs, and the fluorescence intensities decreased further with increasing TCs concentrations (Figure S1). The TC/CDs interaction affects the excitation and emission processes and produces different fluorescence patterns. As shown in Figure S9, the relative fluorescence response variations I/I_0 of the four TCs are different, indicating that the sensor array can be used for TCs identification.

3.4. Optimization of the detection conditions

The next step was the optimization of detection conditions to obtain the best sensor performance. Therefore, fluorescence response experiments with QR-CDs and CPC-CDs were carried out at different excitation wavelengths. The maximum emission wavelength for QR-CDs was obtained with an excitation wavelength of 320 nm, while those for CPC-CDs were obtained at 340 nm and 380 nm, respectively

(Figure S4). By selecting various excitation wavelengths for testing, 370 nm is finally chose as excitation wavelength for CPC-CDs, because it has a more sensitive response (Figure S10). This excitation wavelength also showed a strong and stable emission wavelength. Furthermore, the reaction time of the sensing process was studied. Figure S11, S12 shows that it took only 2 min to achieve stable fluorescence quenching responses upon adding the TCs.

3.5. Sensor array data analysis assisted by LDA and SVM

Figure S9 shows the fluorescence response pattern of the four TCs (1.0 μM) obtained with the sensor array. For each antibiotic, the fluorescence responses of the sensor array were tested five times, resulting in a training matrix of 2 CDs × 4 TCs × 5 replicates.

LDA was used to convert the training matrix into canonical factors. Factor 1 accounts for 59.65% of total data variability, while factor 2 accounts for 40.35%. These two factors were used to generate a two-dimensional diagram in which each point represents the fluorescence response of the two CDs to each antibiotic (Figure 2a). The four TCs were clearly divided into four clusters, and the classification accuracy of each antibiotic was 100%, indicating the effectiveness of the CDs-based sensor array. The identification ability was tested further using antibiotics at different concentrations (10 μM, 25 μM, 50 μM, 100 μM, 150 μM). At each concentration, the investigated antibiotics could be separated from each other, and identified with 100% accuracy (Figure 2b-f). In addition, each of the four TCs in concentrations of 1.0 μM,

10 μM, 25 μM, 50 μM, 100 μM and 150 μM can be completely separated into six plots without overlap (Figure 3). Then, 47 unknown single antibiotics in different concentrations were analyzed and correctly identified, and it was verified that the sensor array had a good predictability.

Subsequently, SVM was used to further analyze and process the data of this experiment. The Radial Basis Function (RBF) kernel was used as the kernel function for SVM. Known samples were applied as training data set to obtain the hyperplane with the largest interval, in order to classify the known samples. As shown in Figure 4, the four TCs could clearly be divided into four clusters without overlap at the concentration of 1.0 μM -150 μM. The classification accuracy of each antibiotic was 100%. In order to test the predictive performance of SVM, 47 unknown antibiotic samples were analyzed using SVM. All samples were correctly identified.

3.6. Differentiation of binary TCs mixtures with LDA and SVM processing

The sensor system was able to differentiate between the binary mixtures of TC and DOX, each mixtures having an antibiotic concentration of 25 μM. The molar ratios of the binary mixtures were 0/100, 20/80, 40/60, 50/50, 100/0, respectively. The LDA and SVM diagram presented in Figure 5 shows that all sample groups with different proportions of the two antibiotics can be completely separated from each other. After training the sensor array, 5 samples with unknown compositions could be identified with 100% accuracy by both LDA and SVM.

3.7. Evaluation of the applicability of SVM

The aforementioned results show that the ideal classification results are both obtained by using SVM and LDA. Both the analysis of a single TCs at various concentrations and the analysis of binary mixtures, SVM shows accurate classification and excellent prediction ability, proving that SVM is feasible in distinguishing and identifying the four TCs. SVM is a reliable machine learning method which is more suitable to deal with classification problems in processing small sample amounts. It has a wider range of applications in classification problems, including not only linear fractional data sets, but also linear non-fractional data sets and nonlinear data. Based on these advantages, SVM is expected to enhance the potential of array sensing detection to process various types of data, and provides researchers with a novel and alternative data analysis method.

3.8. Selectivity

In order to evaluate the selectivity and the anti-interference ability of the fluorescence sensor array, a series of ions that generally exist in real aqueous samples, including Ca^{2+}, Cu^{2+}, Cd^{2+}, Mg^{2+}, Zn^{2+}, Hg^{2+}, Ag^{+}, Na^{+}, Ba^{2+}, Li^{+}, SMM, TOB, AMK, ENR were tested. The concentrations were kept at 10 μM. These substances did not change the fluorescence of the sensing system (Figure S13), while the addition of the four TCs (10 μM) to these solutions resulted in a significant quench of the fluorescence intensity. Figure 6 shows that the four TCs and the other substances can be well separated from each other. The presence of the interfering substances had a

negligible effect on the fluorescence detection, indicating excellent selectivity and anti-interference ability.

3.9. Distinguishing TCs in real samples

In order to explore practical applications of CDs fluorescence sensor array, TCs in milk and river water were determined, respectively. The milk samples were pretreated according to the above methods, then the four TCs with total concentrations of 25 μM and 50 μM were added to the samples for detection. Subsequently, TCs in river water at concentration of 50 μM were tested. In the presence of different antibiotics, distinct responses were generated from the sensor array and further analyzed using LDA and SVM. Figure 7, S14-17 show that the four antibiotics can be divided into four separate groups, indicating the sensor array's potential to identify TCs in real samples. Moreover, 20 unknown samples were distinguished with 100% accuracy.

4. Conclusions

A dual-channel fluorescence sensor array was fabricated and extended the applications of CDs in sensing detection for four TCs (TC, OTC, MTC, DOX) determination based on two carbon quantum dots. Due to the distinct fluorescence response pattern of each TCs, the quantitative detection of TCs is realized by monitoring the change in CDs fluorescence intensity. Through applications of machine learning methods such as LDA and SVM, four TCs can be effectively

differentiated at 1.0 μM. In addition, the sensor array can effectively differentiate the individual TCs and binary mixtures. The sensor array shows high sensitivity, adequate anti-interference, and ability to detect TCs in complex media, such as river water and milk. Moreover, the recognition accuracy was 100% for unknown samples. More importantly, SVM, for the first time, was empolyed and evaluated in the field of array sensing detection, showing the same performance as LDA. Considering the unique features of SVM, the application of SVM provides a novel choice for array sensing systems in processing various types of data. The study demonstrates the potential of the fluorescence sensor array in environmental monitoring and antibiotic quantification.

Funding

Key Technologies Research and Development Program (2016YFC0501205, 2016YFC0501208 and 2017YFD0200706), National Natural Science Foundation of China (21775163).

Acknowledgements

This work was financially supported by the program of National key R & D Program of China (2016YFC0501205, 2016YFC0501208 and 2017YFD0200706), National Natural Science Foundation of China (21775163).express their deep thanks.

References

[1] F. Arcudi, L. Dordevic, M. Prato, Design, Synthesis, and Functionalization Strategies of Tailored Carbon Nanodots, Accounts of Chem. Res. 52(8) (2019) 2070-2079.

[2] Z. Wang, C. Xu, Y.X. Lu, X. Chen, H.T. Yuan, G.Y. Wei, G. Ye, J. Chen, Fluorescence sensor array based on amino acid derived carbon dots for pattern-based detection of toxic metal ions, Sensor Actuat. B-Chem. 241 (2017) 1324-1330.

[3] S. Qu, X. Wang, Q. Lu, X. Liu, L. Wang, A Biocompatible Fluorescent Ink Based on Water-Soluble Luminescent Carbon Nanodots, Angew. Chem. Int. Edit. 51(49) (2012) 12215-12218.

[4] T. Prathumsuwan, P. Jaiyong, I. In, P. Paoprasert, Label-free carbon dots from water hyacinth leaves as a highly fluorescent probe for selective and sensitive detection of borax, Sensor Actuat. B-Chem. 299 (2019) 126936-126947.

[5] D. Bharathi, R.H. Krishna, B. Siddlingeshwar, D.D. Divakar, A.A. Alkheraif, Understanding the interaction of carbon quantum dots with CuO and Cu2O by fluorescence quenching, J. Hazard. Mater. 369 (2019) 17-24.

[6] S. Sun, K. Jiang, S. Qian, Y. Wang, H. Lin, Applying Carbon Dots-Metal Ions Ensembles as a Multichannel Fluorescent Sensor Array: Detection and Discrimination of Phosphate Anions, Anal. Chem. 89(10) (2017) 5542-5548.

[7] Y.L. Wang, P.J. Ni, S. Jiang, W.D. Lu, Z. Li, H.M. Liu, J. Lin, Y.J. Sun, Z. Li, Highly sensitive fluorometric determination of oxytetracycline based on carbon dots and Fe3O4 MNPs, Sensor Actuat. B-Chem. 254 (2018) 1118-1124.

[8] D.Y. Long, J.D. Peng, H.J. Peng, H. Xian, S.Y. Li, X. Wang, J. Chen, Z.Y. Zhang, R.X. Ni, A quadruple-channel fluorescent sensor array based on label-free carbon dots for sensitive detection of tetracyclines, Analyst 144(10) (2019) 3307-3313.

[9] L. Cao, X. Wang, M. J. Meziani, F. Lu, H. Wang, P. G. Luo, Y. Lin, B. A. Harruff, L. M. Veca, D. Murray, S. Y. Xie, Y. P. Sun, Carbon dots for multiphoton bioimaging, J. AM. CHEM. SOC. 129(37) (2007) 11318-11319.

[10] L. Cao, S. Sahu, P. Anilkumar, C.E. Bunker, J. Xu, K.A.S. Fernando, P. Wang, E.A. Guliants, K.N. Tackett, Y.P. Sun, Carbon Nanoparticles as Visible-Light Photocatalysts for Efficient CO2 Conversion and Beyond, J. Am. Chem. Soc. 133 (13) (2011) 4754-4757.

[11] S. Chen, C.H. Xu, Y.L. Yu, J.H. Wang, Multichannel fluorescent sensor array for discrimination of thiols using carbon dot-metal ion pairs, Sensor Actuat. B-Chem. 266 (2018) 553-560.

[12] S. Abbasi-Moayed, M.R. Hormozi-Nezhad, M. Maaza, A multichannel single-well sensor array for rapid and visual discrimination of catecholamine neurotransmitters, Sensor Actuat. B-Chem. 296 (2019) 126691-126700.

[13] F. Ghasemi, M.R. Hormozi-Nezhad, Determination and identification of nitroaromatic explosives by a double-emitter sensor array, Talanta 201 (2019) 230-236.

[14] M. Zhao, H. Yu, Y. He, A dynamic multichannel colorimetric sensor array for highly effective discrimination of ten explosives, Sensor Actuat. B-Chem. 283 (2019) 329-333.
[15] Y. Li, X. Liu, Q. Wu, J. Yi, G. Zhang, Discrimination and detection of benzaldehyde derivatives using sensor array based on fluorescent carbon nanodots, Sensor Actuat. B-Chem. 261 (2018) 271-278.
[16] H. Yu, H. Yang, A direct LDA algorithm for high-dimensional data - with application to face recognition, Pattern Recogn. Lett. 34(10) (2001) 2067-2070.
[17] P. Yan, X. Li, Y. Dong, B. Li, Y. Wu, A pH-based sensor array for the detection and identification of proteins using CdSe/ZnS quantum dots as an indicator, Analyst 144(9) (2019) 2891-2897.
[18] L.L. Li, X. Zhao, M.L. Tseng, R.R. Tan, Short-term wind power forecasting based on support vector machine with improved dragonfly algorithm, J. Clean Prod. 242 (2020).
[19] S.J. Hua, Z.R. Sun, A novel method of protein secondary structure prediction with high segment overlap measure: Support vector machine approach, J. Mol. Biol. 308(2) (2001) 397-407.
[20] S.J. Hong, S.M. Weiss, Advances in predictive models for data mining, Pattern Recogn. Lett. 22(1) (2001) 55-61.
[21] J.G. Ha, H. Moon, J.T. Kwak, S.I. Hassan, M. Dang, O.N. Lee, H.Y. Park, Deep convolutional neural network for classifying Fusarium wilt of radish from unmanned aerial vehicles, J. Appl. Remote Sens. 11 (2017) 042621-1~14.
[22] W.Y. Li, J.C. Zhu, G.C. Xie, Y.K. Ren, Y.Q. Zheng, Ratiometric system based on graphene quantum dots and Eu3+ for selective detection of tetracyclines, Anal. Chim. Acta. 1022 (2018) 131-137.
[23] S.K. Anand, U. Sivasankaran, A.R. Jose, K.G. Kumar, Interaction of tetracycline with L-cysteine functionalized CdS quantum dots - Fundamentals and sensing application, Spectrochim. Acta. A 213 (2019) 410-415.
[24] H. Miao, Y.Y. Wang, X.M. Yang, Carbon dots derived from tobacco for visually distinguishing and detecting three kinds of tetracyclines, Nanoscale 10(17) (2018) 8139-8145.
[25] B.Y. Du, F. Wen, X.D. Guo, N. Zheng, Y.D. Zhang, S.L. Li, S.G. Zhao, H.M. Liu, L. Meng, Q.B. Xu, M. Li, F.D. Li, J.Q. Wang, Evaluation of an ELISA-based visualization microarray chip technique for the detection of veterinary antibiotics in milk, Food Control 106 (2019) 29252-29260.
[26] Y.Y. Wu, P.C. Huang, F.Y. Wu, A label-free colorimetric aptasensor based on controllable aggregation of AuNPs for the detection of multiplex antibiotics, Food Chem. 304 (2020) 125377-125384.
[27] Z. Rouhbakhsh, A. Verdian, G. Rajabzadeh, Design of a liquid crystal-based aptasensing platform for ultrasensitive detection of tetracycline, Talanta 206 (2020).

[28] P. Kowalski, Capillary electrophoretic method for the simultaneous determination of tetracycline residues in fish samples, J. Pharmaceut Biomed. 47(3) (2008) 487-493.
[29] B. Zheng, T. Liu, M.C. Paau, M. Wang, Y. Liu, L. Liu, C. Wu, J. Du, D. Xiao, M.M.F. Choi, One pot selective synthesis of water and organic soluble carbon dots with green fluorescence emission, Rsc Adv. 5(15) (2015) 11667-11675.
[30] Z.D. Gao, S.Y. Wang, Z.J. Xu, M.Y. Liu, Y.F. Huang, S.W. Hu, X.Q. Ren, Synthesis of novel cationic carbon dots and application to quantitative detection of K+ in human serum samples, New J. Chem. 43 (2019) 17937-17940.
[31] W. Wei, J. He, Y. Wang, M. Kong, Ratiometric method based on silicon nanodots and Eu3+ system for highly-sensitive detection of tetracyclines, Talanta 204 (2019) 491-498.
[32] N.R. Ha, I.P. Jung, S.H. Kim, A.R. Kim, M.Y. Yoon, Paper chip-based colorimetric sensing assay for ultra-sensitive detection of residual kanamycin, Process. Biochemi. 62 (2017) 161-168.
[33] N.R. Ha, I.P. Jung, I.J. La, H.S. Jung, M.Y. Yoon, Ultra-sensitive detection of kanamycin for food safety using a reduced graphene oxide-based fluorescent aptasensor, Sci. Rep-Uk. 7 (2017).
[34] H. Li, L. Zhang, B. Huang, X. Zhou, Cost-sensitive dual-bidirectional linear discriminant analysis, Informa. Sciences. 510 (2020) 283-303.
[35] H. Arahmane, A. Mahmoudi, E.M. Hamzaoui, Y. Ben Maissa, R.C. El Moursli, Neutron-gamma discrimination based on support vector machine combined to nonnegative matrix factorization and continuous wavelet transform, Measurement 149 (2020).
[36] Y. Hu, Z. Gao, Sewage sludge in microwave oven: A sustainable synthetic approach toward carbon dots for fluorescent sensing of para-Nitrophenol, J. hazard. mater. 382 (2020) 121048-121055.
[37] Y. Wu, X. Liu, Q. Wu, J. Yi, G. Zhang, Carbon Nanodots-Based Fluorescent Turn-On Sensor Array for Biothiols, Anal. Chem. 89(13) (2017) 7084-7089.
[38] Y.F. Guan, B.C. Huang, C.Qian, H.Q. Yu, Technology, Quantification of Humic Substances in Natural Water Using Nitrogen-Doped Carbon Dots, Environ. Sci. Technol. 51 (2017) 14092-14099.
[39] L.H. Ding, H. M. Yang, S.G. Ge, J.H. Yu, B. Spectroscopy, Fluorescent carbon dots nanosensor for label-free determination of vitamin B 12 based on inner filter effect, Spectrochim. Acta. A 193 (2018) 305-309.
[40] Y.L. Wang, P.J. Ni, S. Jiang, W.D. Lu, Z. Li, H.M. Liu, J. Lin, Y.J. Sun, Z. Li, Highly sensitive fluorometric determination of oxytetracycline based on carbon dots and Fe3O4 MNPs, Sensor. Actuat. B-Chemi. 254 (2018) 1118-1124.
[41] G.L. Li, H.L. Fu, X.J. Chen, P.W. Gong, G. Chen, L. Xia, H. Wang, J.M. You, Y.N. Wu, Facile and Sensitive Fluorescence Sensing of Alkaline Phosphatase Activity with Photoluminescent Carbon Dots Based on Inner Filter Effect, Anal. Chem. 88(5) (2016) 2720-2726.

[42] H. Liu, M. Li, Y. Xia, X. Ren, A Turn-On Fluorescent Sensor for Selective and Sensitive Detection of Alkaline Phosphatase Activity with Gold Nanoclusters Based on Inner Filter Effect, Acs. Appl. Mater. Inter. 9(1) (2017) 120-126.
[43] G. Gao, Y.W. Jiang, H.R. Jia, J.J. Yang, F.G. Wu, On-off-on fluorescent nanosensor for Fe 3+ detection and cancer/normal cell differentiation via silicon-doped carbon quantum dots, Carbon 134 (2018) 232-243
[44] Y. Fan, L. Liu, D.L. Sun, H.Y. Lan, T.M. Yang, Y.B. She, C. Ni, "Turn-off" fluorescent data array sensor based on double quantum dots coupled with chemometrics for highly sensitive and selective detection of multicomponent pesticides, Anal. Chim. Acta. 916 (2016) 84-91.

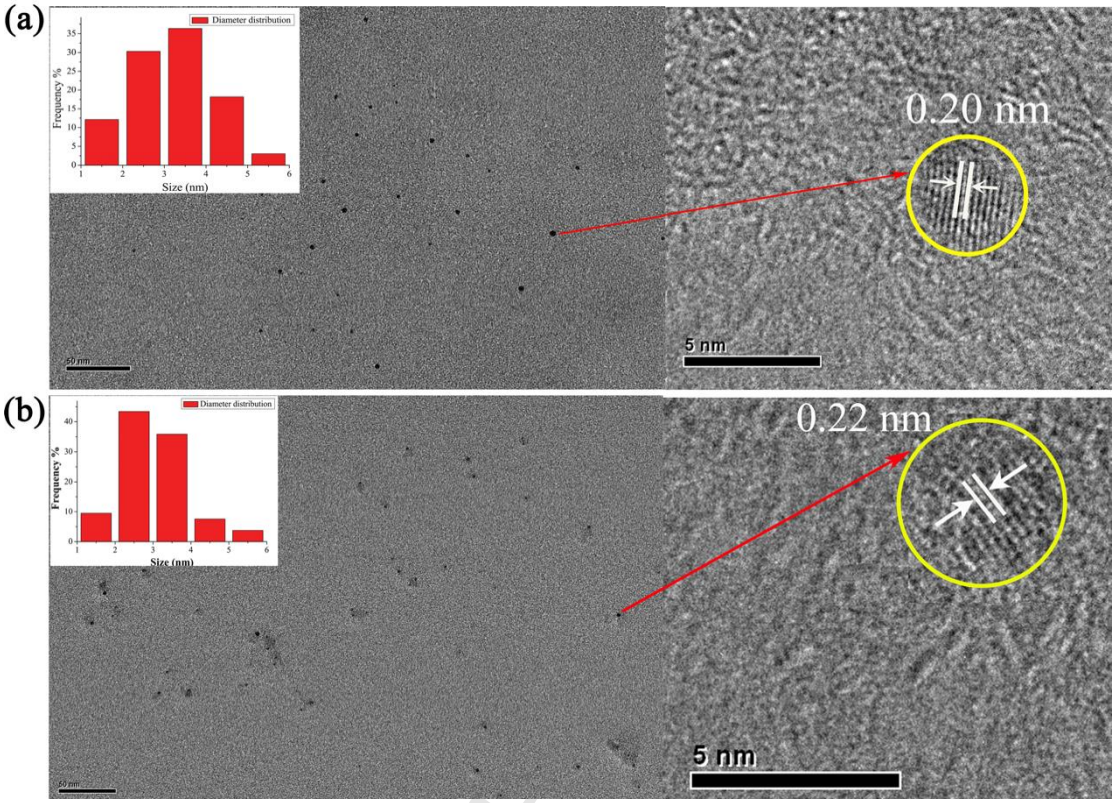

Figure 1. (a) TEM and HRTEM images of QR-CDs (Inset: size distribution of QR-CDs); (b) TEM and HRTEM images of CPC-CDs (Inset: size distribution of CPC-CDs)

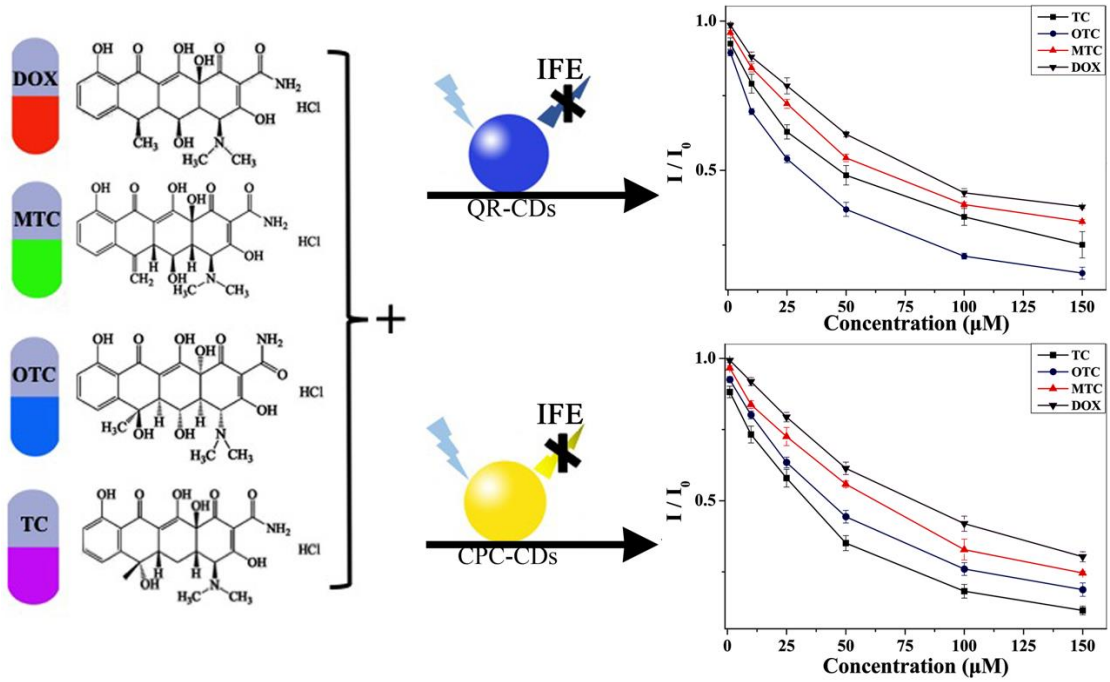

Scheme 1. Mechanism of the sensor array for detecting TCs.

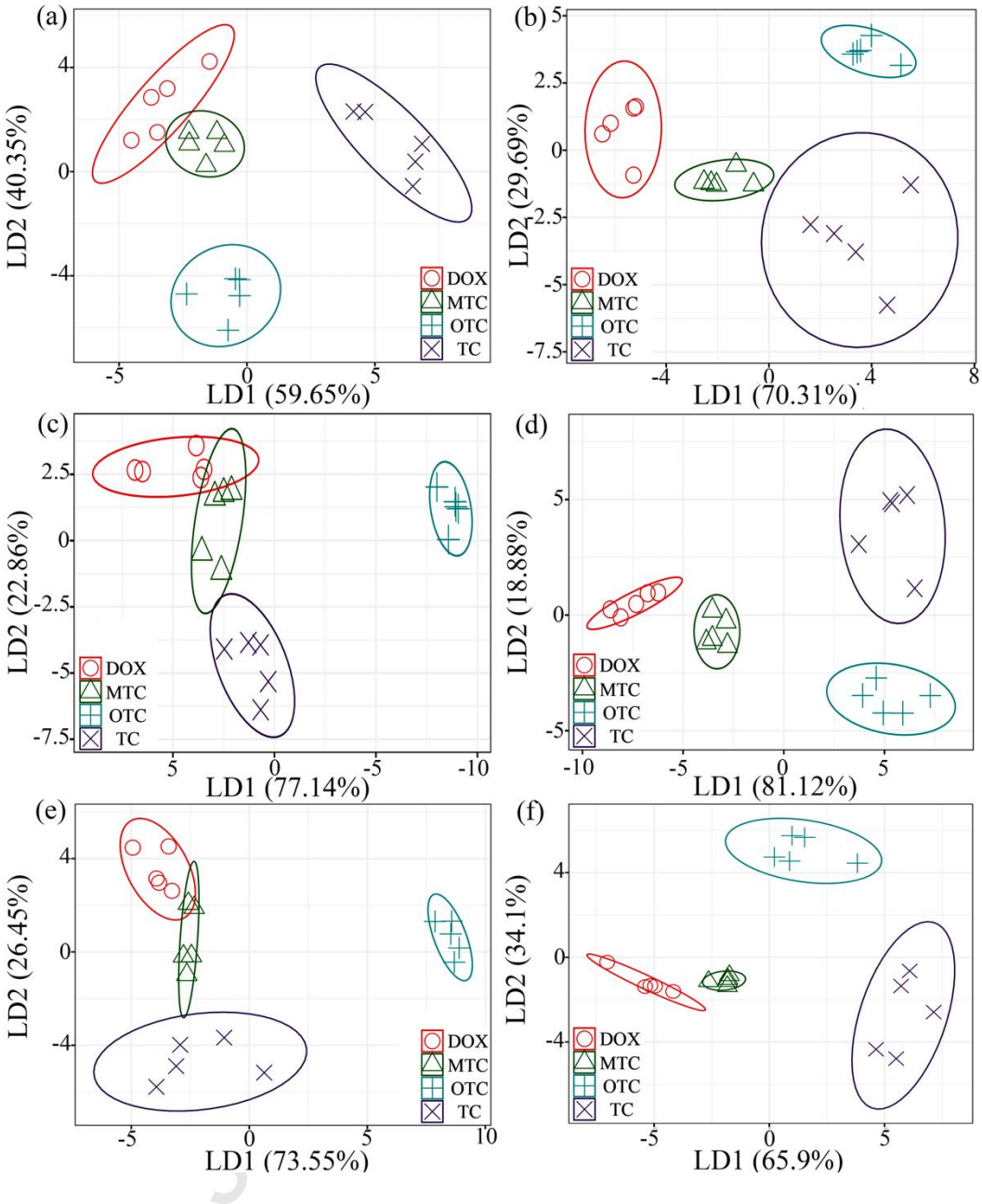

Figure 2. Two-dimensional LDA score plot of the fluorescence sensor array for the discrimination of the four TCs at different concentrations: (a) 1.0 μM; (b) 10 μM; (c) 25 μM; (d) 50 μM; (e)100 μM; (f)150 μM. (QR-CDs, 13.3 μg mL^{-1}; CPC-CDs, 60 μg mL^{-1})

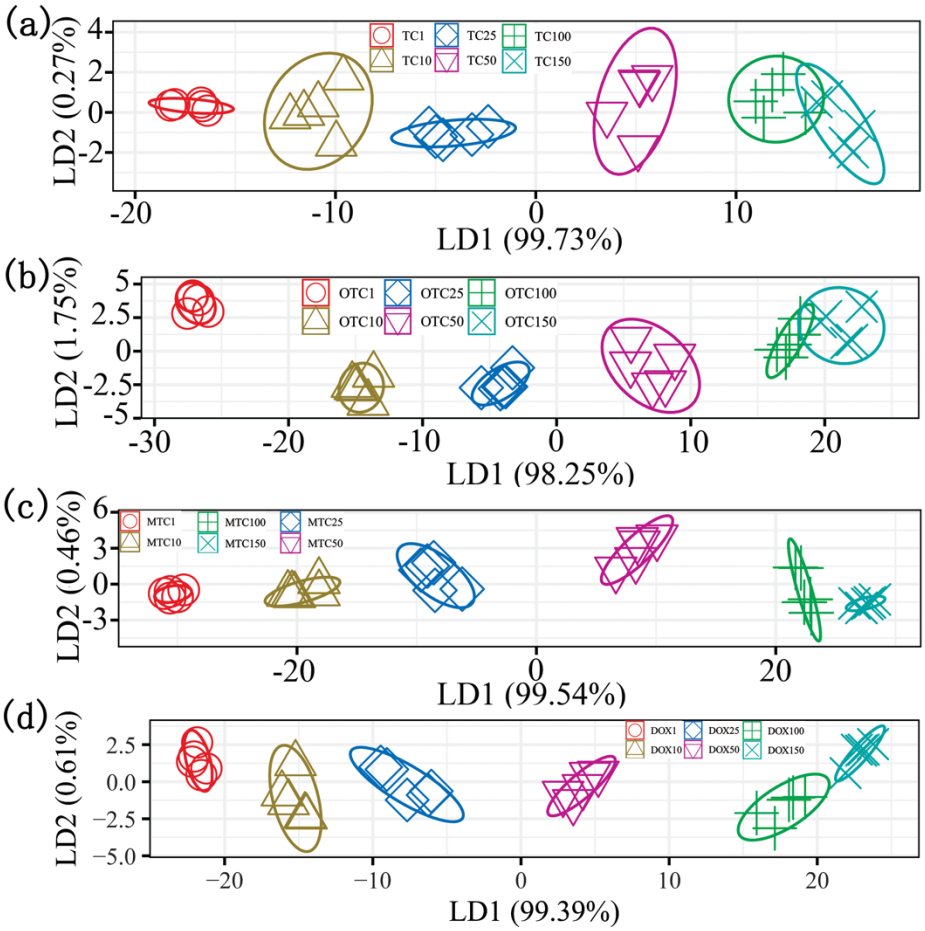

Figure 3. Identification of the four TCs (a) TC; (b) OTC; (c) MTC; (d) DOX at various concentrations (1.0 μM, 10 μM, 25 μM,50 μM 100 μM, 150 μM) by using QR-CDs and CPC-CDs.

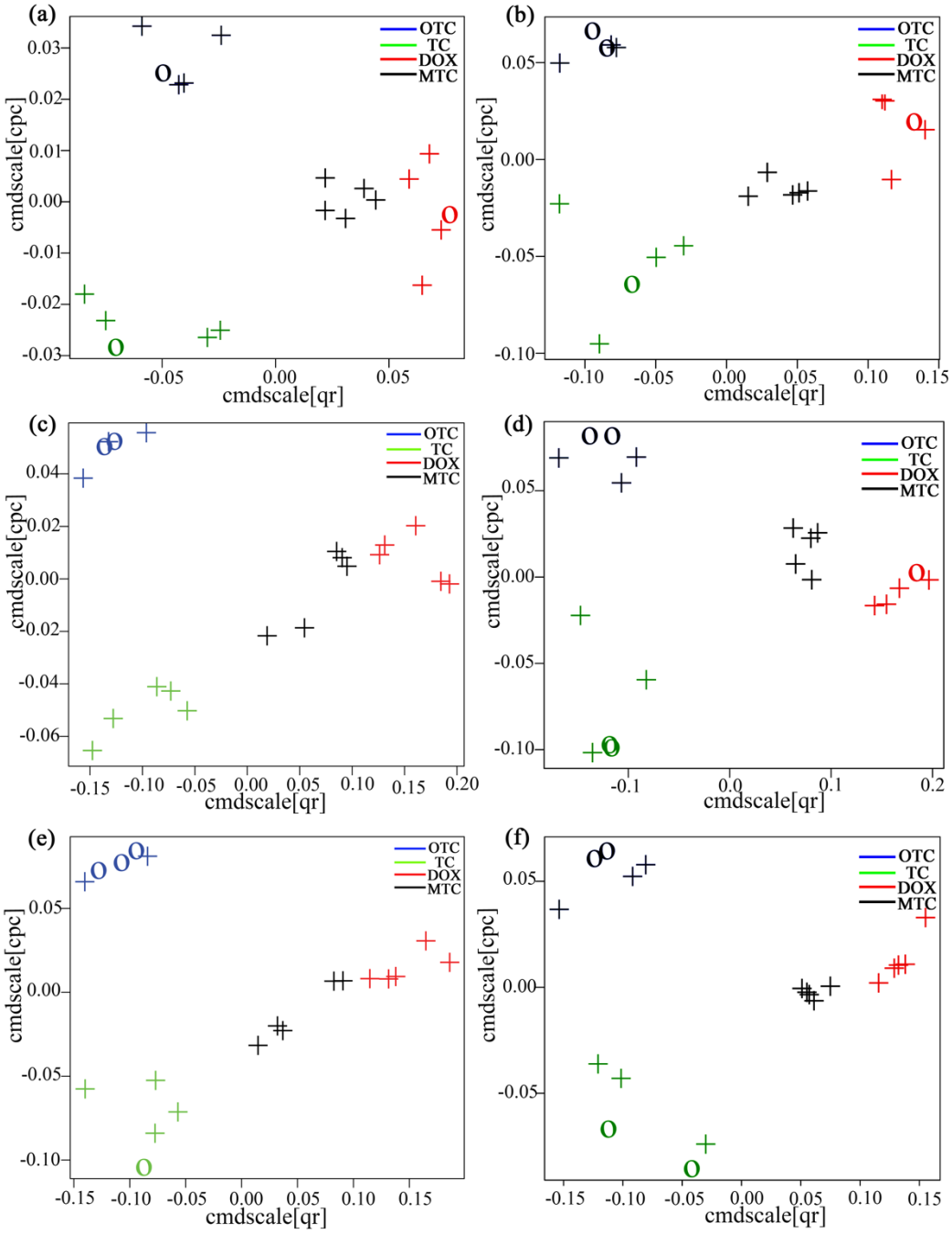

Figure 4. Two-dimensional SVM diagram of the fluorescence sensor array for the discrimination of the four TCs at different concentrations: (a) 1.0 μM; (b) 10 μM; (c) 25 μM; (d) 50 μM; (e) 100 μM; (f) 150 μM. In figure 4, "+" represents the support vector and the "O" represents the sample point.

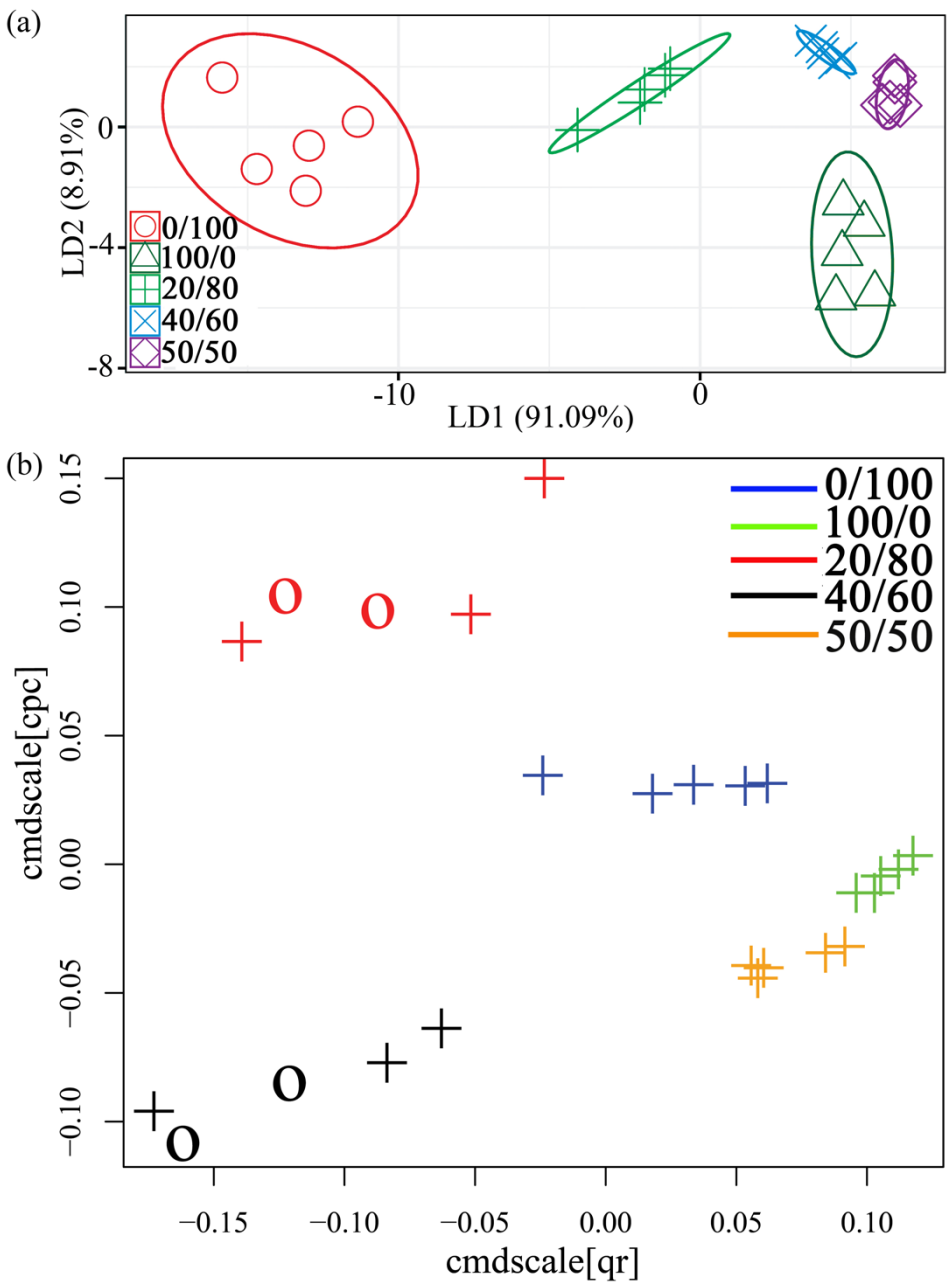

Figure 5. Two-dimensional diagram of the fluorescence sensor array for the discrimination of the mixtures of TC and DOX at different molar ratios (total concentration at 25 μM: (a) LDA; (b) SVM. In figure 5(b), "+" represents the support vector and the "O" represents the sample point.

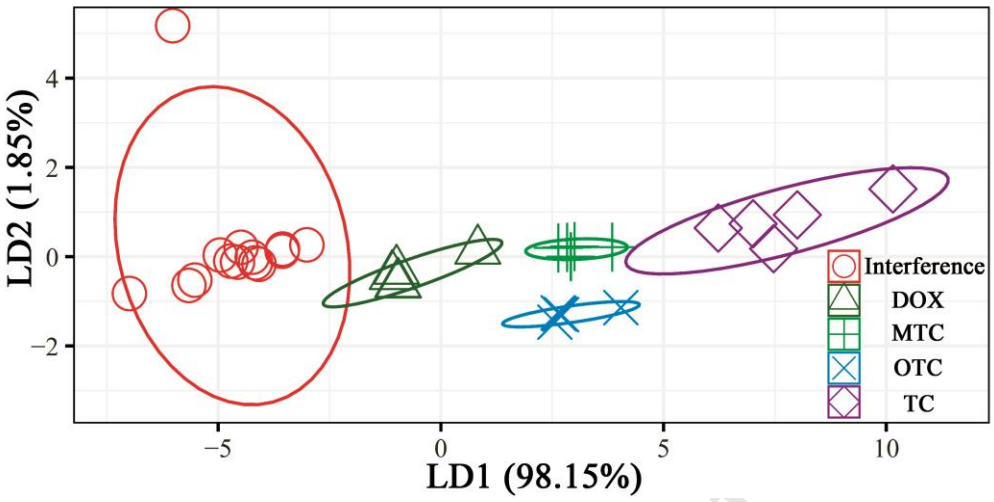

Figure 6. Two-dimensional LDA score plot for the discrimination of the four TCs and other interfering substances based on the fluorescence sensor array (the concentration of the four TCs and the interfering substances including Ca^{2+}, Cu^{2+}, Cd^{2+}, Mg^{2+}, Zn^{2+}, Hg^{2+}, Ag^{+}, Na^{+}, Ba^{2+}, Li^{+}, SMM, TOB, AMK and ENR were all 10 μM).

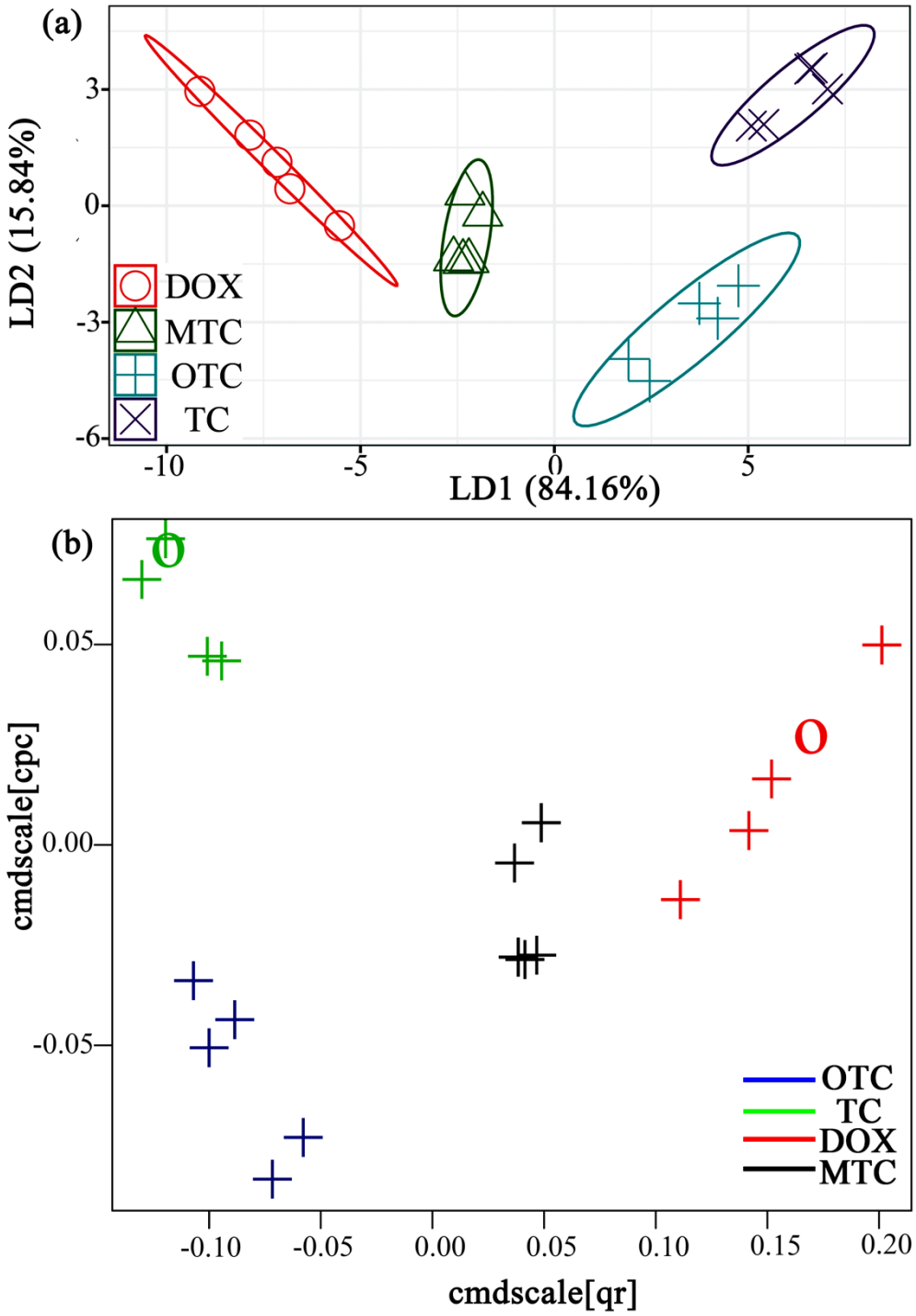

Figure 7. Two-dimensional diagram of the fluorescence sensor array for the discrimination of the real sample (river) at the concentration of 50 μM: (a) LDA; (b) SVM. In figure 7(b), "+" represents the support vector and the "O" represents the sample point.

Declaration of interests

☒ The authors declare that they have no known competing financial interests or personal relationships that could have appeared to influence the work reported in this paper.

☐The authors declare the following financial interests/personal relationships which may be considered as potential competing interests:

Credit Author Statement

Zijun Xu: Conceptualization, Methodology, Software, Writing - Original Draft

Zhaokun Wang: Writing - Original Draft, Validation, Formal analysis, Investigation

Mingyang Liu: Software

Binwei Yan: Formal analysis

Xueqin Ren: Writing - Review & Editing, Supervision

Zideng Gao: Writing - Review & Editing, Supervision

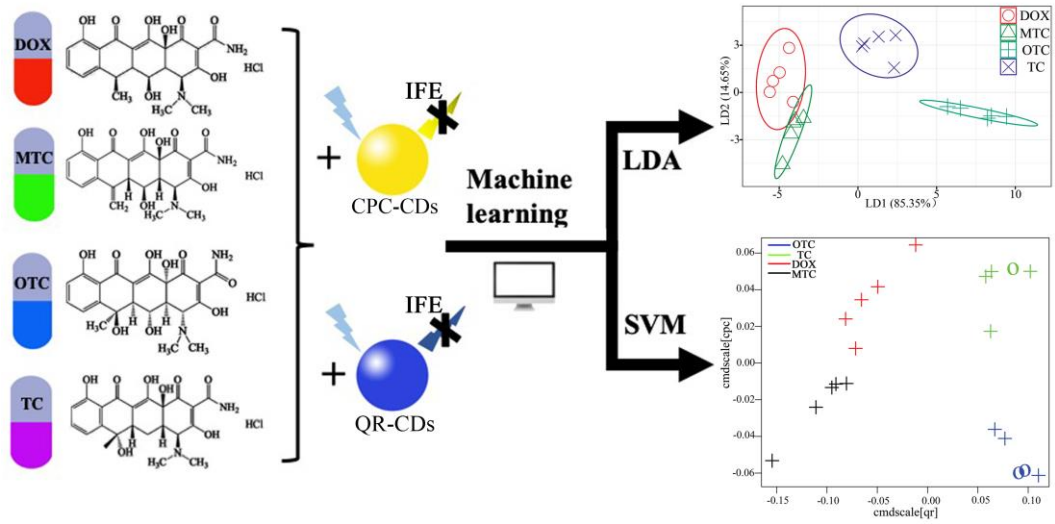

Graphical abstract

Highlights

- Building carbon quantum dots (CDs) for the determination of four tetracyclines based on IFE mechanism
- Fabricating and validating two channel fluorescence sensor array
- SVM processing was employed and evaluated for the first time during array sensing detection